AIMS Materials Science, 11(5): 858–881.
DOI: 10.3934/matersci.2024042
Received: 16 May 2024
Revised: 22 August 2024
Accepted: 02 September 2024
Published: 08 October 2024

http://www.aimspress.com/journal/Materials

Research article

Behavior of shallow concrete beams strengthened using low-cost GCSM and mechanical anchors

Phromphat Thansirichaisree[1], Hisham Mohamad[2], Mingliang Zhou[3], Ali Ejaz[4], Panumas Saingam[5], Qudeer Hussain[6] and Suniti Suparp[7,*]

[1] Thammasat Research Unit in Infrastructure Inspection and Monitoring, Repair and Strengthening (IIMRAS), Faculty of Engineering, Thammasat School of Engineering, Thammasat University Rangsit, Klong Luang, Pathumthani, Thailand
[2] Civil & Environmental Engineering Department, Universiti Teknologi PETRONAS, Seri Iskandar, Malaysia
[3] Key Laboratory of Geotechnical and Underground Engineering of Minister of Education and Department of Geotechnical Engineering, College of Civil Engineering, Tongji University, Siping Road 1239, Shanghai 200092, China
[4] National Institute of Transportation, National University of Sciences and Technology (NUST), Islamabad, Pakistan
[5] Department of Civil Engineering, School of Engineering, King Mongkut's Institute of Technology Ladkrabang, Bangkok 10520, Thailand
[6] Civil Engineering Department, Kasem Bundit University, Thailand
[7] Department of Civil and Environmental Engineering, Srinakharinwirot University, Nakhonnayok, Thailand

* **Correspondence:** Email: suniti@g.swu.ac.th.

Abstract: This study aimed to evaluate the shear strengthening capabilities of reinforced concrete (RC) shallow beams constrained by externally bonded glass chopped strand mat (GCSM) sheets and metallic mechanical anchors. The research investigated the effectiveness of GCSM sheets, known for their cost-effectiveness, ease of installation, and absence of specialized labor requirements, in improving the shear capacity, energy dissipation, and deformation capacity of RC beams. Experimental results revealed that GCSM sheets significantly enhanced the deformation capability, ultimate shear strength, and energy dissipation of RC shallow beams. Beams with GCSM applied to

both the sides and bottom (SB) configuration demonstrated higher load-bearing capacity and energy dissipation compared to beams with GCSM only on the sides. The incorporation of a metallic mechanical bolt anchorage (MBA) system reduced the load-carrying capacities of beams with SB and beams with GCSM applied to only side by 28% and 5%, respectively, due to the drilling required for installation. However, the MBA system significantly improved the deflection performance, with beam B-S-A (GCSM on sides only and supplemented with MBA exhibiting the highest ultimate deflection of 23.92 mm. Overall, beams equipped with the MBA system showed superior ultimate deflection compared with those without it. Despite some reductions in load-bearing capacity, GCSM sheets combined with MBA systems proved highly effective in enhancing the shear strength, energy dissipation, and deformation capabilities of RC shallow beams, making them a valuable alternative for shear strengthening applications.

Keywords: RC shallow beams; shear strengthening; glass chopped strand mat fiber; confinement configuration; metallic mechanical bolt anchorage system; load-deflection responses

1. Introduction

The demand for restoration, strengthening, and rehabilitation of existing reinforced concrete (RC) structures has significantly expanded during the past few years. Building and bridge structures may need to be strengthened due to an increase in load demand and/or the degradation of strength owing to material deterioration. Moreover, in seismically-prone countries, the use of low-strength concrete and insufficient reinforcing details may cause older and already-existing structures to perform poorly during seismic events. Buildings and civil structures are susceptible to damage from earthquakes, and over time, maintenance and repair work are often necessary [1]. Strategically located on the Eurasian Plates, Thailand is constantly at risk for earthquakes, which can cause damage in cities closer to the epicenter. In their research, Ornthammarath and Warnitchai [2] examined numerous structures that lacked seismic design and came to the conclusion that these structures lacked adequate shear reinforcement, which was the primary factor in catastrophic shear failure. In order to ensure the safety of people and property during upcoming extreme events, such shear-deficient beams must be strengthened.

Numerous studies have already been carried out on the enhancement of shear capabilities of RC beams by employing various techniques, such as external jacketing and the use of innovative materials [3–6]. However, such materials have drawbacks, including intensive labor demands and an increase in weight and volume. Additionally, there are issues with corrosion and the handling of heavy steel plates with steel jacketing [7].

Fiber-reinforced polymer (FRP) composites can be used to alleviate these limitations. Different configuration types, mechanical anchors, novel materials, and wrapping techniques have also been examined to improve shear capacity and delay the debonding process in externally bonded FRP RC beams [8–11]. Synthetic fiber FRP composites, like glass FRP and carbon FRP, are frequently used since they possess advantageous characteristics, including corrosion resistance, high stiffness, and low weight [12]. Several other beneficial alternative composite materials have also been designed, such as polyethylene terephthalate, engineered cementitious composite (ECC) matrix [13], and geosynthetic cementitious composite material [14,15]. Externally wrapped FRP composites have

proved to be feasible in enhancing the strength, energy dissipation, and ductility of strengthened members [5]. Glass chopped strand mat (GCSM) fiber polymers have recently been used in concrete with brick waste aggregate [16] and in RC deep beams [17]. These GCSM displayed exceptional performance in the enhancement of ductility and shear strength of RC deep beams. Joyklad et al. [16] utilized fiber chopped mat stands in recycled aggregate concrete to enhance its properties. Results concluded that, in comparison to the corresponding control specimens, ultimate strain enhancement in low-, medium-, and high-strength recycled aggregate concrete was 320%, 308%, and 294%, respectively. Lam et al. [17] strengthened RC deep beams utilizing GCSM on low- and high-strength concrete beams. According to the results, with the same configuration of GCSM compared to specimens without GCSM, the ultimate load-carrying capacity of low- and high-strength concrete beams increased by 70% and 108%, respectively. However, most research efforts have been linked to FRP strengthening on RC deep beams [18,19]. Although all these approaches and methodologies have demonstrated higher gains in the shear capacity of RC beams, only limited studies were reported on RC shallow beams [20,21]. There is no research on the behavior of shallow RC beams that are externally constrained by GCSM fiber. Testing RC shallow beam specimens is necessary for improving their shear performance and ensuring optimal use of GCSM materials.

Considerable research has been done on RC deep beams confined by GCSM, and the literature has been updated with regard to their confinement behavior. On the other hand, the use of GCSM applied externally to RC shallow beams needs to be thoroughly investigated, as well as the effectiveness and structural performances of this approach in the enhancement of shear capacity. According to the author's knowledge, no previous research has been carried out on the shear behavior of concrete constrained with these GCSM sheets. Moreover, prior studies found that almost all beams strengthened with externally bonded FRP techniques failed, mainly due to the debonding of fiber composite from the concrete surfaces, with the exception of the beams with entirely wrapped FRP, which failed because of ruptured fibers [22,23]. The debonding failure mechanism of the fiber composite from the FRP to the concrete interface manifested itself in a brittle manner, which occurred immediately after the ultimate strength was attained. The entire capability of the fiber sheet is not fully utilized with such a mechanism of failure. In the past, different types of anchoring systems were investigated for steel bars and concrete beams [24,25]. To prevent delamination failure and improve the effectiveness of FRP laminates, different anchoring systems, such as mechanical bolt anchoring (MBA), were examined and recommended [26,27]. However, the FRP laminates were found unsuitable for use with mechanical bolts, as the laminates lacked sufficient bearing strength to withstand the forces applied by the fastened bolts [28]. Lam et al. [17] enhanced the shear capacity of RC beams using CGSM sheets and utilized MBA and epoxy-based anchors. The rupture of CGSM was observed in the presence of anchors, highlighting the effectiveness of MBA. Saingam et al. [29] enhanced the flexural behavior of brick masonry walls with ferrocement overlays. The debonding of ferrocement overlays was effectively delayed by the presence of MBA. Some previous research on GCSM strengthening revealed that there is an issue with bond failure between GCSM and concrete surface [17,30–33]. Therefore, MBA systems, as suggested by Lam et al. [17], were used in this research to avoid premature GCSM sheet failure as a result of the MBA system's higher efficiency compared to other anchorage systems.

This research intends to assess the shear performance of two GCSM-confinement setups for RC shallow beams and to investigate the efficiency of GCSM confinement in enhancing the shear and deformation capacity of concrete shallow beams. The effect of the MBA system in preventing the

premature failure of GCSM sheet is also the purpose of this research. Responses of a total of five RC shallow beams with two different confinement configurations and an MBA system were evaluated. In order to develop an in-depth understanding of the behavior of strengthened RC shallow beams employing externally bonded GCSM sheets, we evaluated deflection response, strength enhancement, effect of strengthening configuration, energy dissipation capacity, effect of type of confinement configuration, ultimate failure modes of RC shallow beams, and effect of anchorage.

2. Materials and methods

2.1. Test matrix

In this research work, five shallow RC beams were constructed with two distinct configurations for strengthening and with and without mechanical anchorage. Strengthening was accomplished using GCSM fiber, and anchoring was achieved using mechanical bolt. Table 1 provides information on the test matrix. Control beam (B-CON) is lacking strengthening and mechanical anchorage. In beam with GCSM applied only at sides (B-S) and beam with GCSM applied only at sides and bottom (B-SB), the second letter is for strengthening configuration, i.e., S for sides and GCSM strengthening on the side and bottom. In B-S-A and B-SB-A, the third letter "A" stands for anchoring, indicating that these two specimens also have anchorage in addition to strengthening.

Table 1. Beam nomenclature based on strengthening and anchor.

Type of beams	Strengthening	Strengthening configuration	Metallic anchors
B-CON	Control	None	None
B-S	GCSM	Side only	None
B-SB	GCSM	Side and bottom	None
B-S-A	GCSM	Side only	Yes
B-SB-A	GCSM	Side and bottom	Yes

2.2. Details of beams

Figure 1 depicts the beam's longitudinal and cross-sectional views. All dimensions are displayed in millimeters (mm). Each beam measures 1700 mm in length, 100 mm in width, and 250 mm in depth. A 15 mm concrete cover was provided. Additionally, anchorage was offered to prevent the pullout failure. For the development length, bending of steel reinforcement was given in accordance with ACI 1999. The primary goal of this research was to study the effect of GCSM fiber on the shear capacity of shallow beams. So, there was no shear reinforcing provided, causing beam failure in shear. To prevent local buckling, stirrups were nevertheless placed at the center of the beam 50 mm apart, as detailed in Figure 1.

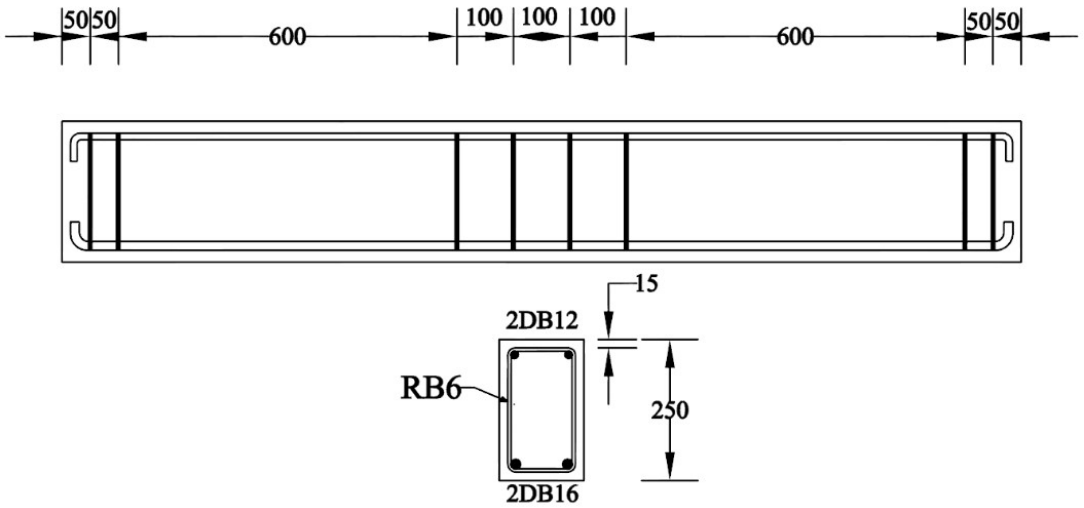

Figure 1. Cross-sectional and longitudinal view (units in millimeters).

2.3. Properties of materials

Table 2 displays the characteristics of the materials employed in this research project. The concrete used for making RC beams has a 28th-day cylindrical strength of 14.58 MPa. A non-woven glass fiber mat created by spreading 50 mm continuous filament roving along with a polyester binder was used for making up the GCSM sheet. The GCSM sheet had a density of 600 g/m^2 and a thickness of 0.5 mm. The ultimate strength of GCSM was 180 MPa. The width of the GCSM roll was 1.0 m. The tensile strength of GCSM was determined using ASTM D3039M [34] and found to be 180 MPa. GCSM used for strengthening is illustrated in Figure 2. The steel bars' tensile characteristics are also displayed in Table 2. Deformed bars (DB) with diameters of 16 and 12 mm were employed for longitudinal tensile reinforcement and compression reinforcement, respectively. As vertical stirrups, round bars (RB) having 6 mm diameter were used. GCSM was applied to the beam via the aid of a two-part epoxy resin consisting of hardener and resin, mixed in a 2:1 ratio. Epoxy resin was supplied by Smart and Bright Company Limited, Thailand, and its physical and mechanical characteristics, as given by the supplier, are shown in Table 3.

Table 2. Material properties.

Material properties	Yielding stress (MPa)	Yielding strain	Ultimate stress (MPa)	Ultimate strain
Concrete Strength	14.58	-	-	-
RB-6	372.7	0.00184	494.7	0.1836
DB-12	633	0.003944	761	0.115137
DB-16	455	0.00241	614	0.015197

Figure 2. Glass chopped strand mat (GSCM) fiber.

Table 3. Properties of epoxy resin.

Properties	Values
Ultimate strain (%)	1
Flexural strength (MPa)	70
Tensile strength (MPa)	120
Curing time (hours)	7–10

2.4. Strengthening configurations

In this study, two different strengthening configurations were used to examine the strengthening impact of GCSM fiber sheet. Beams with only side strengthening are denoted by "S", while beams with bottom and side strengthening are denoted by "SB". Strengthening configuration is also displayed in Figure 3. The concrete beam's surface was roughened with a grinder before the GCSM sheet was applied, and dust was removed with a cloth. After that, a brush epoxy resin was applied to the beam, and the GCSM sheet was carefully fastened onto the concrete beam, in homogeneous contact with the concrete's surface. Figure 4 depicts the entire procedure of surface grinding and applying the GCSM sheet.

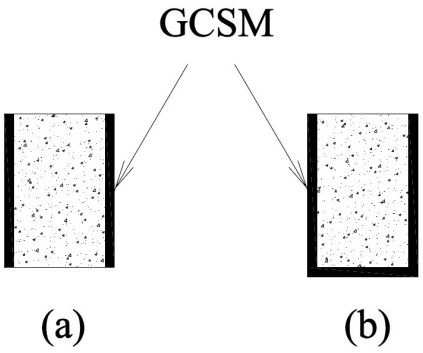

Figure 3. Strengthening configuration of beams: (a) GCSM fiber on sides only, and (b) GCSM fiber on sides and bottom.

Figure 4. RC shallow beams: (a) before GCSM strengthening and (b) GCSM strengthening.

2.5. Low-cost anchorage system

Previous studies on GCSM reinforcement revealed bond failure between GCSM and concrete surfaces [26,27]. In this study, a MBA system was employed to prevent the premature failure of the GCSM sheet. As illustrated in Figure 5, it consisted of a zinc flake–coated anchor, hex-headed bolts with full threads, washers, and nuts along with mechanical expansion anchors measuring 25 mm in length and 7 mm in diameter. Figure 6 displays the strengthened beam's anchorage spacing details. According to Figure 6, the MBA was spaced 75 mm apart vertically, 62 mm apart from the support, and 125 mm apart from the support in the horizontal direction. The anchors were applied only in the shear span region where the shear failure of the control beam was expected to occur. In this study, number and spacing were assumed to cover the shear span region. For the installation of the MBA system, predetermined spacings of 40 mm long and 8 mm wide holes were drilled in the GCSM and beam. When the nut was tightened, the mechanical expansion anchor in the MBA system expanded laterally to generate frictional resistance. To prevent the local rupture of the GCSM, a washer was positioned between the GCSM and the nut.

Figure 5. Expansion anchor, hex-headed bolt, nuts, and washers.

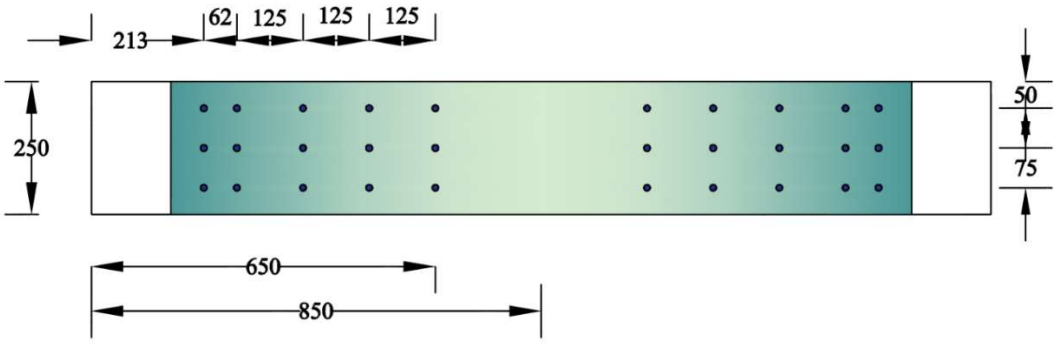

Figure 6. Mechanical bolt anchorage detail for GCSM strengthening on beams (units in millimeters).

2.6. Specimen preparation and strengthening

Figure 7 illustrates the reinforcement employed in the beam. Concrete was mixed mechanically and then poured into a plywood mold to create the RC shallow beams, as depicted in Figure 8. After the curing period, beams were strengthened by GCSM fiber sheet. Two beams were strengthened from the sides and two beams were strengthened from the sides and bottom. Figure 9 illustrates the RC shallow beams after strengthening. Following the process of strengthening, a MBA system was installed on two beams: one beam with GCSM sheet on the sides, and one beam with GCSM sheet on the sides and bottom. The MBA system installed on RC-strengthened beams is depicted in Figure 10.

Figure 7. Beam reinforcement view.

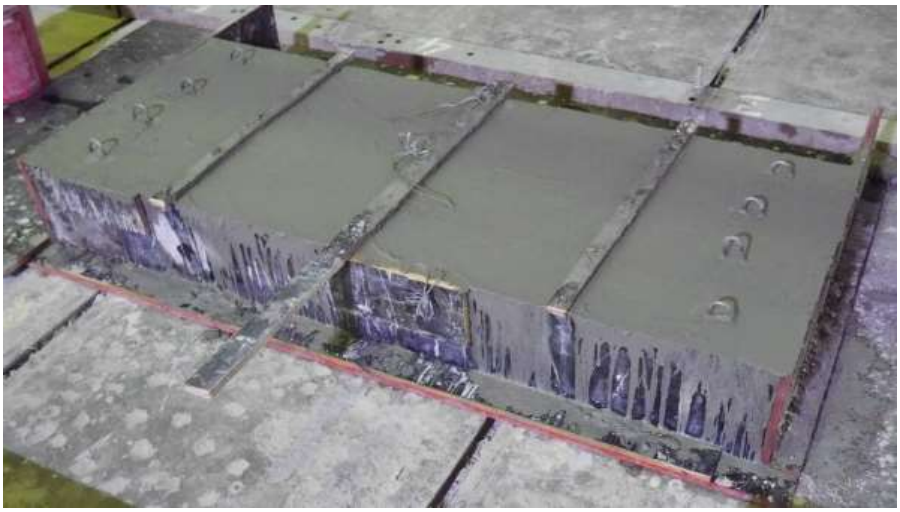

Figure 8. RC beam construction.

Figure 9. GCSM sheet strengthening of RC beams.

Figure 10. MBA system for strengthened beams.

2.7. Instrumentation and loading setup

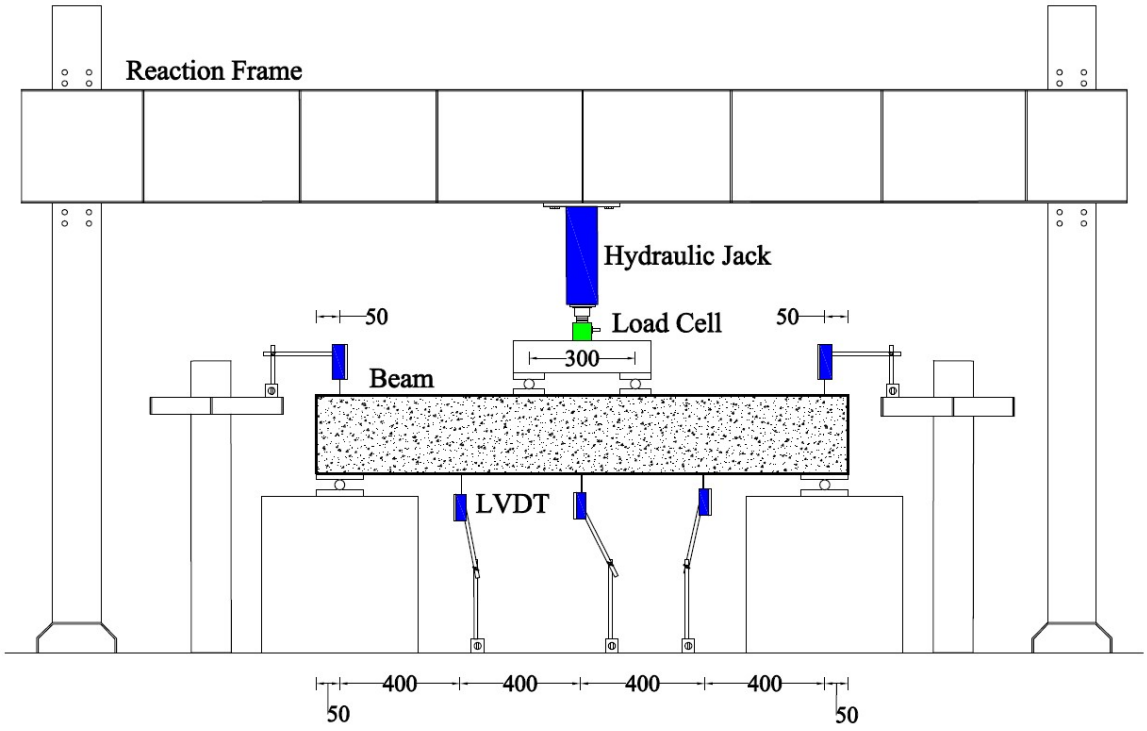

Figure 11. Setup for three-point load testing of RC beams (units in millimeters).

The testing apparatus presented in Figure 11 shows four-point loads applied to the beams. One strain gauge was also affixed to the center of each tension and compression steel bar. Reaction frame, hydraulic jack, and load cell each had a load-carrying capacity of 1500, 600, and 500 kN, respectively. Three linear variable displacement transducers (LVDT) were employed to measure the downward deformation of the RC beams. Moreover, one LVDT was employed at each end of the beam to measure the RC beams' upward deformation. Figure 12 represents the loading setup used in the

laboratory for testing RC beams. All beam specimens were tested in the normal environmental conditions of Thailand. The average temperature was 35 °C. Average humidity was approximately 78%–80%.

Figure 12. Testing setup in laboratory.

3. Results and discussion

The beams were subjected to load in the testing setup shown in Figure 12, and deflection was also measured at that time. During testing, beam failure modes were also investigated. Table 4 displays the ultimate load and deflection of all tested beams. As shown in Table 4, results indicate that GCSM confinement significantly improved the shear capacity and ductility of beams. The "B-SB" beam showed maximum increase in ultimate load. The increment in ultimate load over B-CON beam was 134%. In comparison to B-CON, the ultimate deflection increased by 57% and 81% in B-S and B-SB, respectively. Comparing confinement configurations revealed that GCSM-equipped beams with both the sides and the bottom performed better than those with GCSM exclusively on the sides.

The increment in ultimate load and ultimate deflection for the B-SB beam was 134% and 81%, respectively, as compared to the B-S beam, owing to more confinement provided in the former. The provision of anchorage has further enhanced the ductility of beams, according to the data in Table 4. The B-S-A beam experienced the highest increase in final deflection. In comparison to B-CON, B-S-A had an 83% higher ultimate deflection. Moreover, MBA-equipped confined beams showed an increase in ultimate load, but their ultimate load capacity was lower than that of confined beams lacking anchoring. This might be the result of the MBA system beam's drilling impact, which slightly reduced the load capacity. The more precise techniques, such as starting slowly with light pressure and using a smaller drill bit to create a hole in the correct area before using the larger drill bit, could be useful to reduce the adverse effects of anchor bolts. Overall, Table 4's findings made it abundantly evident that GCSM are very effective in enhancing the shear capacity and ductility of RC shallow beams.

Table 4. Experimental results.

Beams	Ultimate load (kN)	Increase in ultimate load (%)	Ultimate deflection (mm)	Increase in ultimate deflection (%)
B-CON	62.82	-	3.75	-
B-S	117.09	86	5.92	57
B-SB	147.12	134	6.80	81
B-S-A	98.99	58	6.89	83
B-SB-A	143.93	129	11.20	198

3.1. Load-deflection behavior

The load-deflection behavior of each tested beam is depicted in Figure 13. It is clear from the graph data that GCSM-confined beams outperformed control beams in terms of performance. The effectiveness of GCSM confinement in enhancing the strength and deformation capacity of RC shallow beams was clearly proven by the results. In comparison to the beam with GCSM on the sides only, confinement of beams by GCSM on the sides and bottom demonstrated better performance. This is attributed to the improved bonding between GCSM and concrete surface. Similar results were also reported by Lam et al. [17] in their research work on GCSM-composite RC beams. The load-deflection graph further highlighted the critical fact that beam deformation increases with GCSM confinement. Normally, the application of confinement reduces the likelihood of shear failure. When the ultimate load was reached, the load-carrying capacity of the control beam and the beams without anchorage suddenly decreased, indicating shear failure in these beams. This is attributable to the delamination of GCSM in beams lacking a MBA system.

GCSM-confined beams with anchorage systems showed distinct behavior from other beams in terms of load-deflection behavior. The load-deflection graph after the maximum load indicated a progressive decrease in load, while the deflection of these beams continued to increase until failure. The MBA system prevents the delamination of GCSM [17] and utilizes the full capacity of GCSM sheets, which is responsible for improving the deformation capacity as well as the ultimate load capacity. In order to increase the shear capacity and ductility of RC beams, GCSM sheets are particularly effective, as shown by the results of load-deformation curves. Furthermore, results also indicated that the MBA system shifted the RC shallow beams' failure behavior from shear failure to flexure failure mode. Furthermore, the load-carrying capacities of the beams with bolts also suddenly decreased due to the sudden shear cracks. These cracks crossed the lines of anchor bolts resulting in a sudden reduction of their anchoring efficiency.

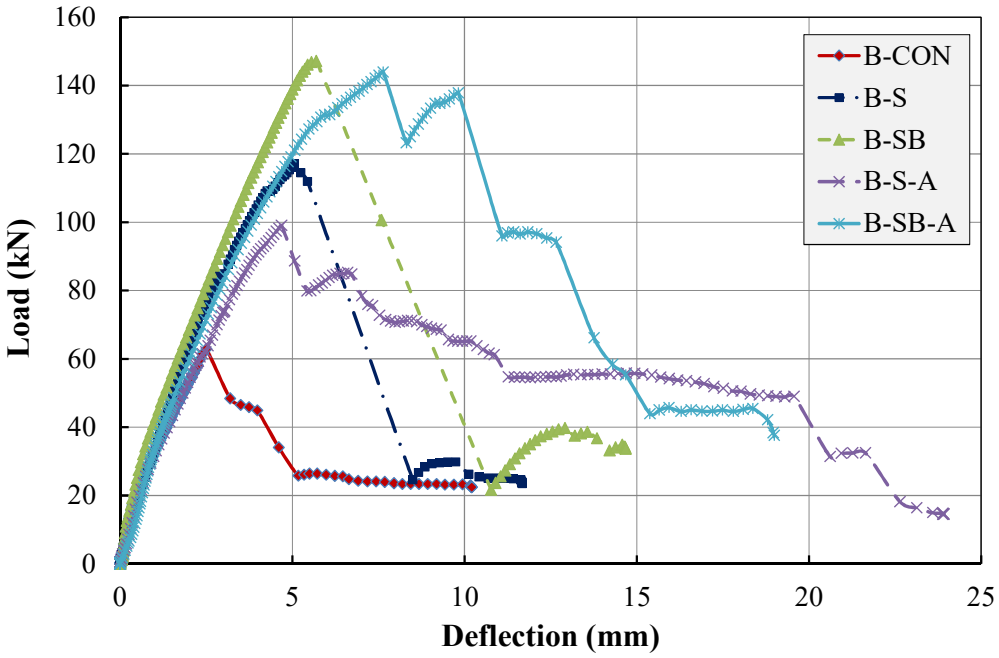

Figure 13. Load-deflection behavior of control and GCSM-confined beams.

3.2. Ends-deflections of beams

Figures 14 and 15 display the deflection at the left and right ends of the beams for all tested beams. From Figure 14 it can easily be deduced that GCSM-confined beams displayed greater left end deflection than the control beam. The control beam had the lowest left-end deflection and failed at a lower load. The effectiveness of GCSM confinement in enhancing the strength and end deformation capacity of RC shallow beams was proven by the results. In comparison to the beam with GCSM on the sides only, confinement of beams by GCSM on the sides and bottom exhibited higher efficacy. The left-end deflection graph also showed the crucial point that the deformation of beams increases with the application of the MBA system. This occurs because beams with MBA systems do not delaminate GCSM. Due to the GCSM sheets on the sides and bottom, as well as the MBA system in that beam, which eventually enhances the load carrying and deformation capability, the B-SB-A beam displayed the highest left-end deflection.

Figure 15 displays the deflection at the right end of each tested beam. Similar to the left-end deflection, right-end deflection of GCSM-confined beams is higher as compared with the control beam. The control beam failed under less strain and had the lowest right-end deflection. Results clearly demonstrated that GCSM confinement enhanced the strength as well as end-deformation capacity of RC shallow beams. In comparison to the beam having GCSM only on the sides, the confinement of beams by GCSM on the sides and bottom showed a greater performance. The right-end deflection graph demonstrated that, in contrast to the left-end deflection, the deformation of beams decreases with the implementation of the MBA system. Due to the GCSM sheets on the sides and bottom, which ultimately enhanced the load carrying and deformation capabilities, the beam B-SB demonstrated the highest right-end deflection and took the highest load.

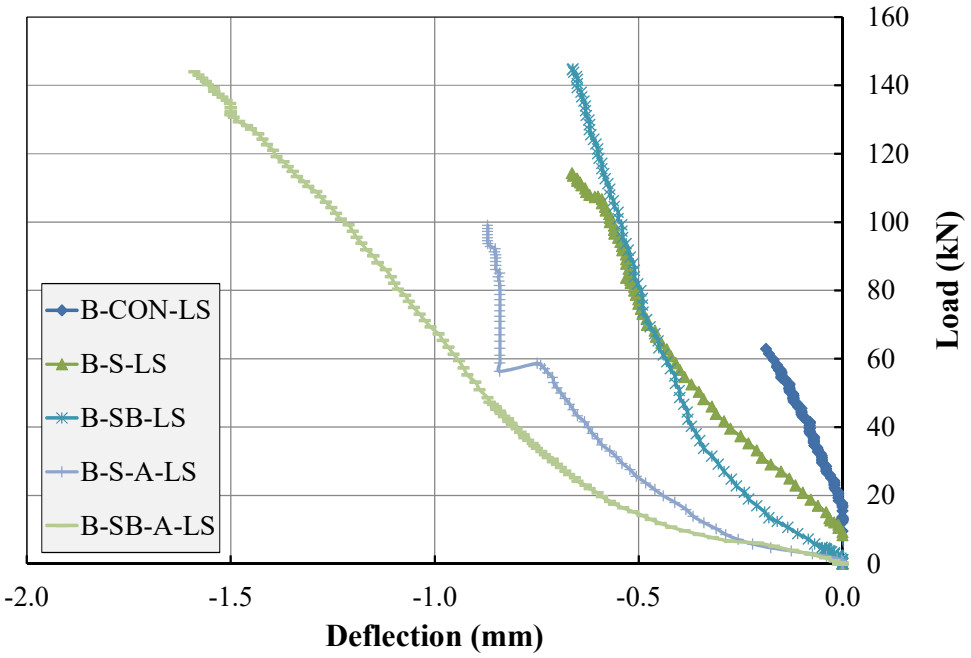

Figure 14. Left-end deflection of control and GCSM-confined beams.

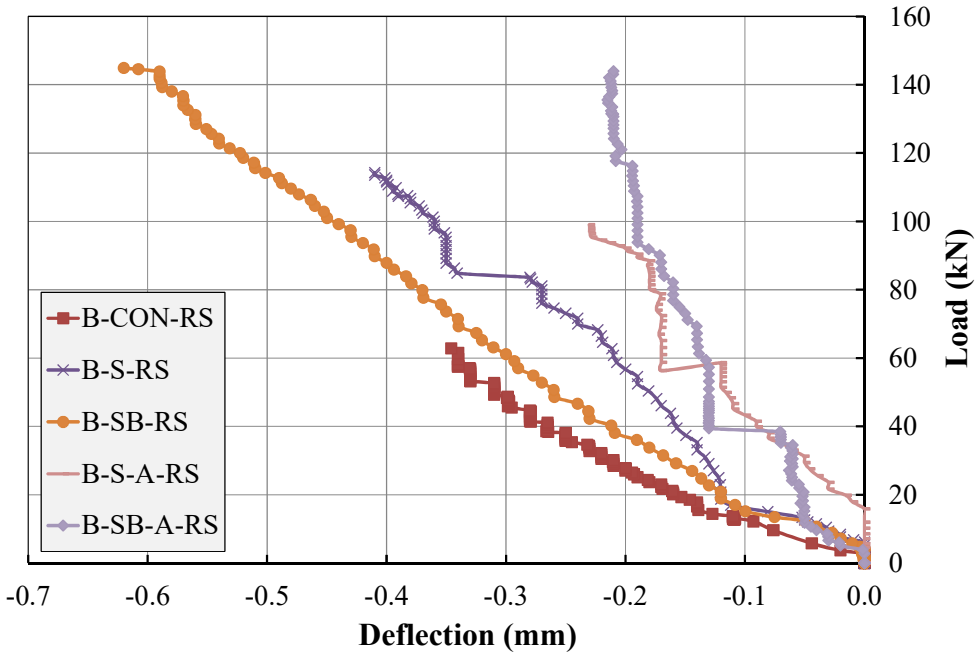

Figure 15. Right-end deflection of control and GCSM-confined beams.

3.3. Energy dissipation capacity of beams

The area under the load-deformation curve was employed to determine the energy dissipation capacity (EDC). The EDC of each tested RC shallow beam is displayed in Table 5. According to the test results, all strengthened beams have considerably higher EDCs than the control beam. The GCSM configuration and MBA system have a considerable impact on the beams' ability to dissipate

energy. The increase in EDC of B-S and B-SB was 107% and 255%, respectively. Nearly 148% more energy can be dissipated by the B-SB beam with GCSM on the sides and bottom than by the beam with GCM merely on the sides. The performance of MBA-equipped beams was superior to all other beams, and they demonstrated an increase in EDC of 325% and 384%, respectively, over the control beam. By preventing premature beam debonding failure, the MBA system enables the beams to exploit the maximum potential of the GCSM sheets.

Table 5. Energy dissipation capacity of beams.

Beams	EDC (kN-mm)	Increase (%)
B-CON	262	----
B-S	542	107
B-SB	931	255
B-S-A	1114	325
B-SB-A	1269	384

3.4. Behavior of tension and compression steel bars

The ultimate strain values of steel bars in tension and compression for each examined specimen are listed in Table 6. Figure 16 also depicts the complete load-strain behavior of tension steel bars of all tested beams. From Table 6 and Figure 16, it can easily be concluded that confined beams have higher ultimate tensile strain values than unconfined beams. The ultimate tensile strain values of GCSM-strengthened B-S and B-SB beams increased by 86% and 126%, respectively. This indicates that GCSM strengthening is effective in enhancing the tensile strain capabilities of tension steel bars, which in turn is linked to higher load-taking capacities of strengthened beams. Moreover, results also revealed that GCSM confinement on the sides and bottom causes 40% higher strain in tensile bars than beams with GCSM confinement only on the sides. Figure 17 also depicts the complete load-strain behavior of compression steel bars for all tested beams. From Table 6 and Figure 17, it can be easily concluded that confined beams have higher ultimate compression strain values than unconfined beams. However, the behavior of the load strain curve for all beams is similar, i.e., a linear load strain curve for compression and tensile steel bars. The increase in ultimate compression strain values of GCSM-strengthened B-S and B-SB beams was 223% and 267%, respectively. Owing to the higher load-bearing capacities of reinforced beams, GCSM strengthening is efficient in improving the compression strain capacity of tension steel bars. By comparison of results, it is apparent that B-SB-A beams, i.e., with side and bottom GCSM strengthening as well as a MBA system, sustain the highest ultimate tensile and compression strain. These outcomes demonstrate the efficiency of the MBA system in enhancing strain-taking capabilities, which ultimately increases the shear capacity of GCSM-strengthened beams.

Table 6. Strain values for steel bars.

Beams	Ultimate tensile strain (mm/mm)	Increase tensile strain (%)	Ultimate compression strain (mm/mm)	Increase compression strain (%)
B-CON	1039	-	–432	-
B-S	1934	86	–1396	223
B-SB	2347	126	–1586	267
B-S-A	2527	143	–1135	163
B-SB-A	2813	171	–1668	286

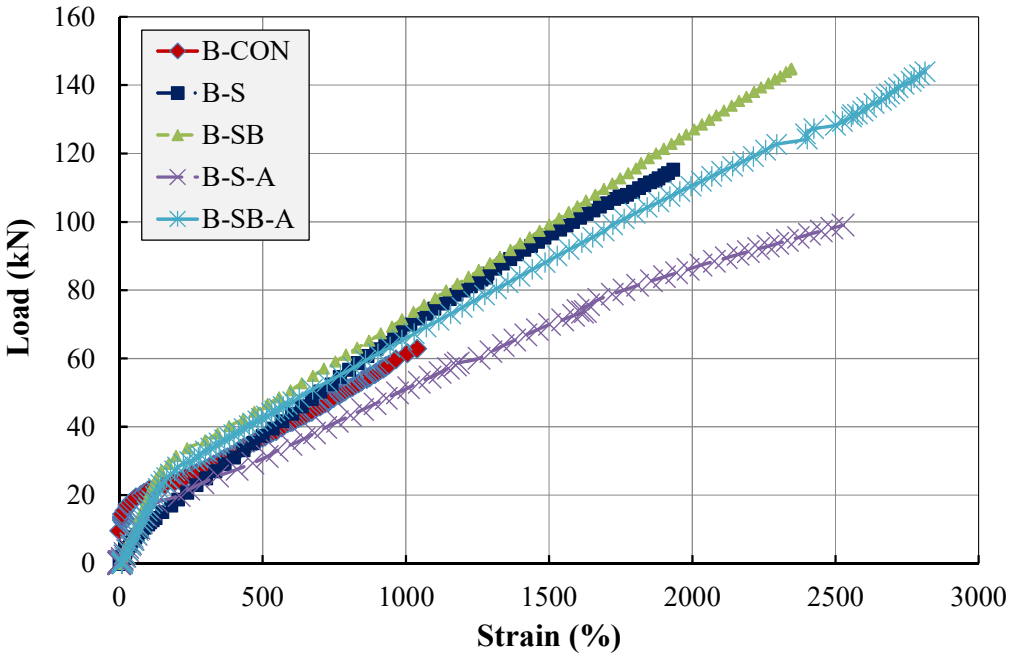

Figure 16. Load strain graph of tension bar.

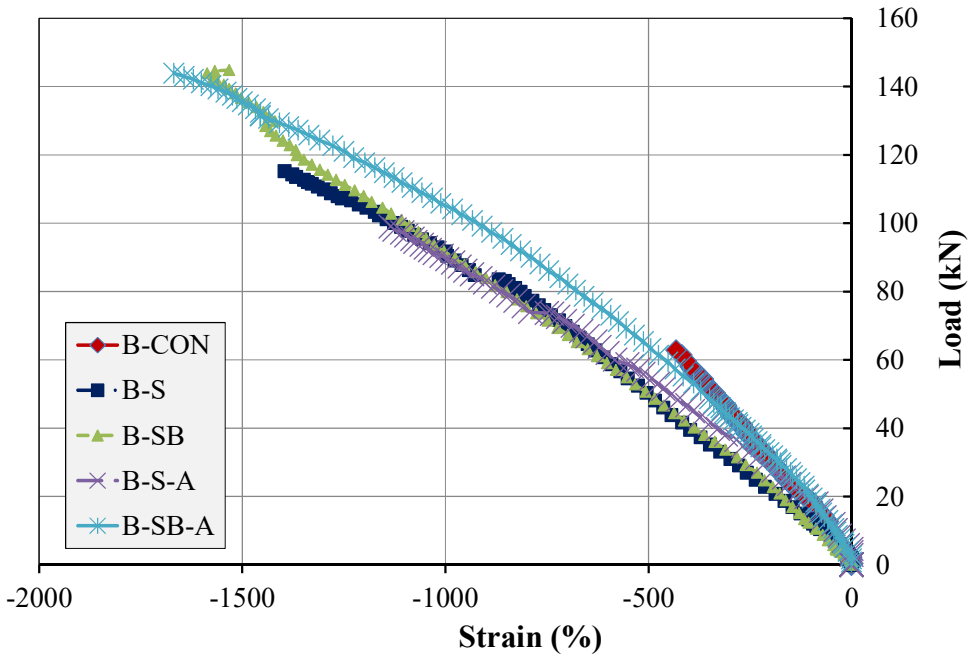

Figure 17. Load strain graph of compression bar.

3.5. Effect of strengthening configuration

Figures 18 and 19 depict the impact of GCSM configuration on the behavior of RC shallow beams. Two distinct GCSM sheet configurations were present on the beams. B-S and B-S-A beams had a GCSM sheet applied solely to their sides, while B-SB and B-SB-A beams had the GCSM sheet applied to both their sides and bottom. From Figure 18, it is clear that beams having GCSM on the sides and bottom have higher load carrying ability than beams having GCSM merely on the sides. These results are in accordance with the research work of Lam et al. [17] on RC deep beams. The ultimate load in the B-SB beam was 48% higher than the B-S beam, while the load in B-SB-A was 71% greater than that of B-S-A. The greater increment is associated with the strong confinement provided by the GCSM sheet on the sides as well as on the bottom of the beam. Figure 19 illustrates the impact of the GCSM configuration on the ultimate beam deflection. As can be observed from the graph, in beams without the MBA system, the B-SB beam had a 30% higher deflection than the B-S beam. On the other hand, in beams with the MBA system, the ultimate deflection decreased by 48% in B-SB-A compared with B-S-A. At the same time, in beams with the MBA system, the ultimate deflection decreased by 115% in B-SB-A compared with B-S-A. The B-S-A beam performed better in terms of deflection, whereas the B-SB beam's performance in carrying load was highest compared with the other confined and unconfined beams.

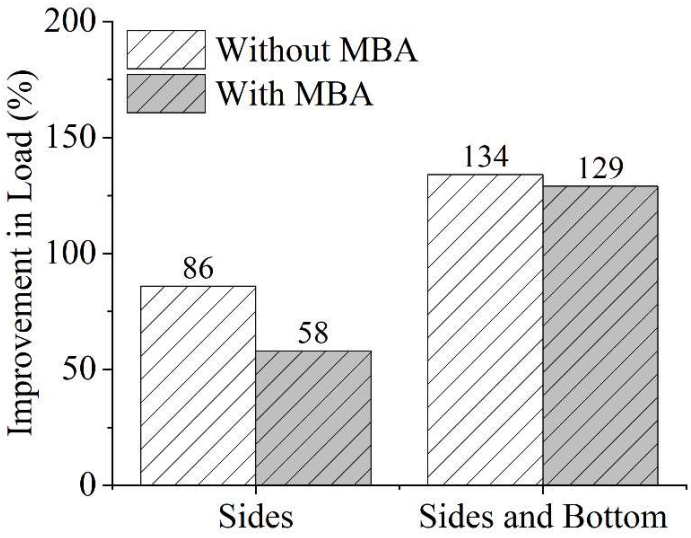

Figure 18. Effect of strengthening configuration on load capacity.

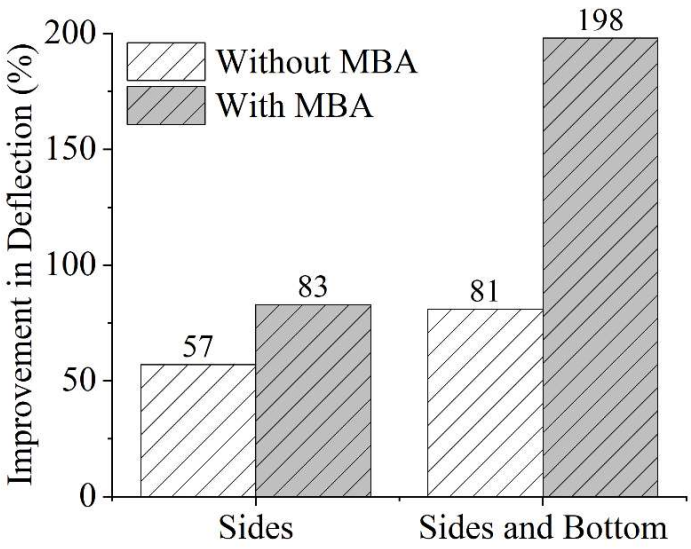

Figure 19. Effect of strengthening configuration on ultimate deflection.

3.6. Effect of anchorage

The effect of the MBA system on load and deflection is represented in Figures 20 and 21, respectively. Figure 20 demonstrates that the MBA system reduces the load-bearing capacities of beams B-S and B-SB for both types of GCSM configuration by 28% and 5%, respectively, primarily due to the drilling of holes in beams for MBA system installation. However, the MBA system significantly enhances beam deflection, which ultimately improves the beams' capacity to dissipate energy. A comparison of results revealed that the MBA system improved the deflection of B-S and B-SB by 57% and 81%, respectively. Data on ultimate deflection indicated that, among all beams, B-S-A had the highest ultimate deflection of 23.92 mm. Overall, beams with MBA systems perform substantially better in terms of ultimate deflection than beams without MBA systems. In addition, the presence of anchors on side and bottom bonded configurations enhanced the maximum tensile and

compression strain of longitudinal steel bars, as shown in Table 6. For instance, the longitudinal tension bar in B-SB-A beam (with anchors) depicted a 45% greater improvement in tension strain, as compared to B-SB beam (without anchors), over that of the control beam.

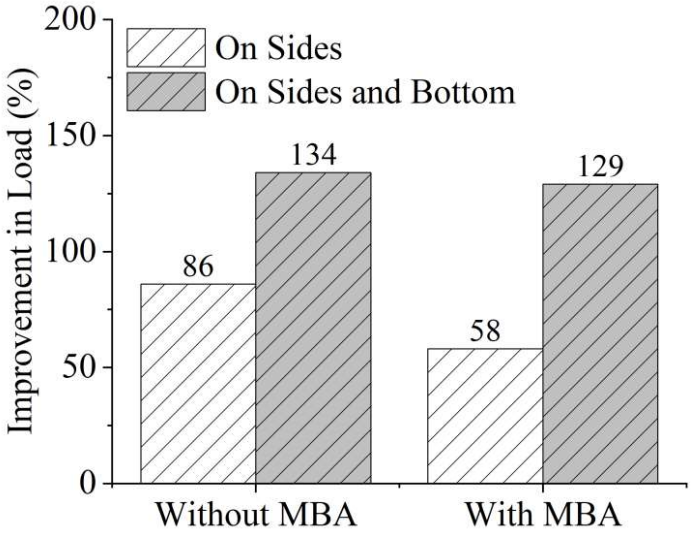

Figure 20. Effect of MBA system on strength.

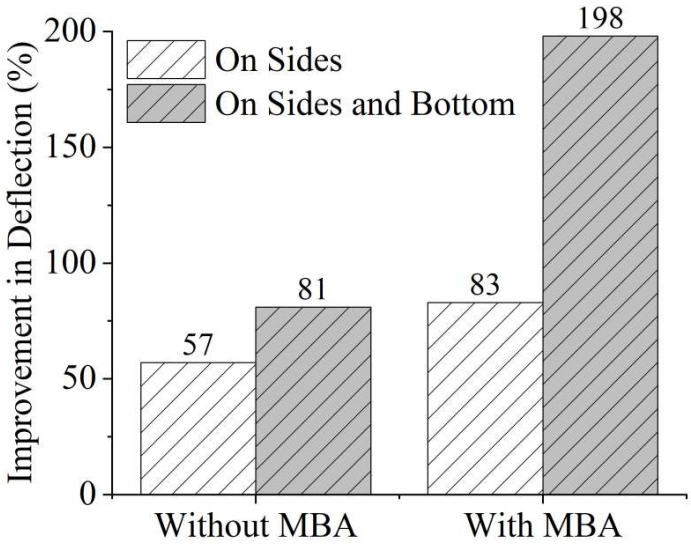

Figure 21. Effect of MBA system on ultimate deflection.

3.7. Failure modes of beams

Figure 22 displays the failure modes of each tested beam. The control beam's initial crack appeared as a flexural crack beneath the right point loading at 37.95 kN load, and then a flexural crack was observed at 38.63 kN load. A new flexural crack was discovered at the center of the beam when the load was increased to 46.10 kN. New cracks appeared as the load increased further, and previous cracks widened. Control beam shear cracks began appearing at a load of 53.54 kN, and at 61.78 kN the beam experienced shear failure damage. In control beams lacking shear reinforcement,

some earlier studies [17,29] have also noted this pattern of shear failure behavior. In beams having GCSM confinement (B-S and B-SB), the debonding of the GCSM sheet can be seen in Figure 22b,c. However, due to the confinement, they failed at higher loads as compared with the control beam. Beams B-S and B-SB failed at a load of 115.22 and 144.74 kN, respectively. MBA system was applied on beams B-S-A and B-SB-A, as can be seen in Figure 22d,e. The MBA system was particularly effective in preventing the debonding of the GCSM sheet from the surface of the beam, as can be seen in Figure 22d,e. In comparison with the control beam, the failure loads for the B-S-A and B-SB-A beams were 58% and 129% higher, respectively. Failure of B-S-A and B-SB-A beams was associated with concrete crushing underneath the loading points. Further, after the tests, the GCSM was removed to see the crack pattern. The observed crack patterns (see Figure 23) were almost identical to the control beam, i.e., B-CON.

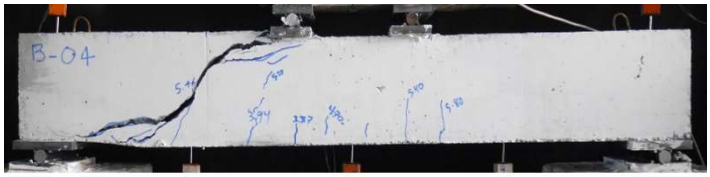

(a) B-CON

(b) B-S

(c) B-SB

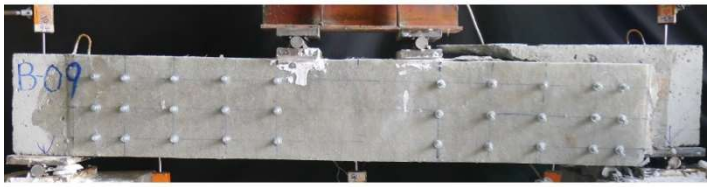

(d) B-S-A

(e) B-SB-A

Figure 22. Ultimate beam failure modes.

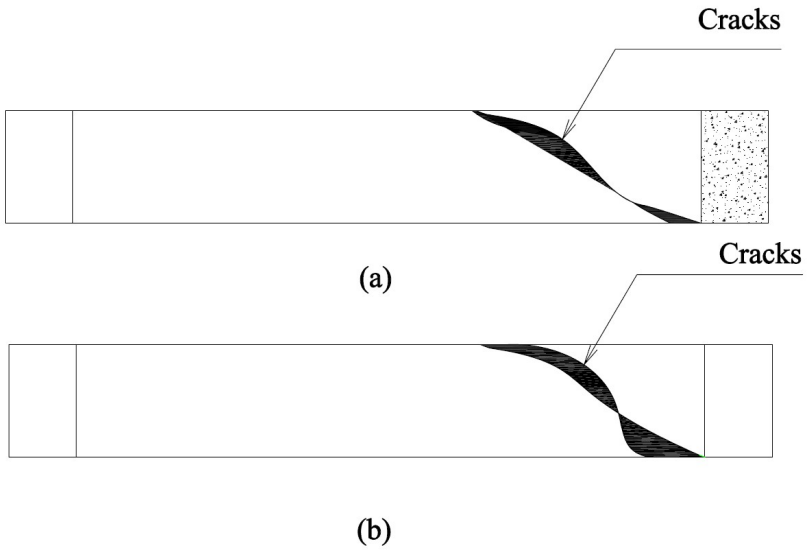

Figure 23. Typical crack patterns in the GCSM-strengthened beams. (a) Beams without anchor and (b) beams with anchors.

4. Conclusions

Through experimental investigation, this research assessed the shear-strengthening behavior of RC shallow beams employing a GCSM sheet. Evaluations included the effects of two different strengthening configurations and MBA system. From the experimental results, the following conclusions can be drawn:

1. The deformation capability, ultimate shear strength, and energy dissipation capability of RC shallow beams are all significantly improved by GCSM sheets.

2. Beams with SB configuration, i.e., GCSM on the sides and bottom, have a higher load-bearing capability as well as energy dissipation than beams with GCSM solely on the sides.

3. The MBA system reduced the load-taking capabilities of B-S and B-SB beams by 28% and 5%, respectively, which is linked to the drilling of holes in the beams for the installation of the MBA system.

4. The MBA system significantly enhanced the deflection of beams. Data on ultimate deflection depicted that, among all beams, B-S-A exhibited the maximum ultimate deflection of 11.2 mm. Overall, beams with the MBA system performed substantially better in terms of ultimate deflection than beams lacking the MBA system.

5. Despite their easy installation and effective results, GCSM sheets are highly beneficial and preferred for shear strengthening of RC shallow beams.

6. It is important to note that only a single configuration of anchors was used in this study. Future studies should extend this work and explore other configurations to reach the optimum anchoring efficiency. Furthermore, the MBA anchoring should be explored when the number of CGSM sheets exceeds one.

Use of AI tools declaration

The authors declare they have not used Artificial Intelligence (AI) tools in the creation of this article.

Acknowledgement

This study was supported by Thammasat University Research Fund, Contract No TUFT 32/2567. Thanks, are also extended to Asian Institute of Technology (AIT), Thailand for supporting test facilities.

Author contributions

Main experimental work and data analysis: P.T; H.M; M.Z; A.E; P.S; Q.H. and S.S; writing—original draft: P.T; H.M; M.Z; A.E; P.S; Q.H. and S.S; writing—review and editing: P.T; H.M; M.Z; A.E; P.S; Q.H. and S.S.

Conflict of interest

The authors declare no conflict of interest.

References

1. Jirawattanasomkul T, Likitlersuang S, Wuttiwannasak N, et al. (2020) Structural behaviour of pre-damaged reinforced concrete beams strengthened with natural fibre reinforced polymer composites. *Compos Struct* 244: 112309. https://doi.org/10.1016/j.compstruct.2020.112309
2. Ornthammarath T, Warnitchai P (2016) 5 May 2014 MW 6.1 Mae Lao (Northern Thailand) earthquake: Interpretations of recorded ground motion and structural damage. *Earthq Spectra* 32: 1209–1238. https://doi.org/10.1193/081814EQS129M
3. Sim J, Park C, Moon DY, et al. (2005) Characteristics of basalt fiber as a strengthening material for concrete structures. *Compos Part B Eng* 36: 504–512. https://doi.org/10.1016/j.compositesb.2005.02.002
4. Yao J, Teng JG, Chen JF, et al. (2005) Experimental study on FRP-to-concrete bonded joints. *Compos Part B Eng* 36: 99–113. https://doi.org/10.1016/J.COMPOSITESB.2004.06.001
5. Ascione L, Feo L (2000) Modeling of composite/concrete interface of RC beams strengthened with composite laminates. *Compos Part B Eng* 31: 535–540. https://doi.org/10.1016/S1359-8368(99)00063-3
6. Katakalos K, Manos G, Papakonstantinou C, et al. (2019) Seismic retrofit of R/C T-beams with steel fiber polymers under cyclic loading conditions. *Buildings* 9: 1–16. https://doi:10.3390/buildings9040101
7. Engindeniz M, Kahn LF, Zureick AH, et al. (2005) Repair and strengthening of reinforced concrete beam-column joints: State of the art. *ACI Struct J* 102: 187–197. https://doi.org/10.14359/14269

8. Chen GM, Teng JG, Chen JF, et al. (2013) Shear strength model for FRP-strengthened RC beams with adverse FRP-steel interaction. *J Compos Constr* 17: 50–66. https://doi.org/10.1061/(asce)cc.1943-5614.0000313
9. Chen JF, Teng JG (2003) Shear capacity of FRP-strengthened RC beams: FRP debonding. *Constr Build Mater* 17: 27–41. https://doi.org/10.1016/S0950-0618(02)00091-0
10. Khalifa A, Nanni A (2000) Improving shear capacity of existing RC T-section beams using CFRP composites. *Cem Concr Compos* 22: 165–174. https://doi.org/10.1016/S0958-9465(99)00051-7
11. Triantafyllou G, Rousakis T, Karabinis A, et al. (2019) Corroded RC beams at service load before and after patch repair and strengthening with NSM CFRP strips. *Buildings* 9: 67. https://doi.org/10.3390/buildings9030067
12. Santarsiero G (2018) FE modelling of the seismic behavior of wide beam-column joints strengthened with CFRP systems. *Buildings* 8: 31. https://doi.org/10.3390/buildings8020031
13. Shang X, Yu J, Li L, et al. (2019) Strengthening of RC structures by using engineered cementitious composites: A review. *Sustainability* 11: 3384. https://doi.org/10.3390/su11123384
14. Jirawattanasomkul T, Kongwang N, Jongvivatsakul P, et al. (2019) Finite element analysis of tensile and puncture be-haviours of geosynthetic cementitious composite mat (GCCM). *Compos Part B Eng* 165: 702–711. https://doi.org/10.1016/J.COMPOSITESB.2019.02.037
15. Hussain Q, Ruangrassamee A, Joyklad P, et al. (2022) Shear enhancement of RC beams using low-cost natural fiber rope reinforced polymer composites. *Buildings* 12: 602. https://doi.org/10.3390/buildings12050602
16. Joyklad P, Saingam P, Ali N, et al. (2022) Low-cost fiber chopped strand mat composites for compressive stress and strain enhancement of concrete made with brick waste aggregates. *Polymers* 14: 4714. https://doi.org/10.3390/polym14214714
17. Lam L, Khan AQ, Pimanmas A, et al. (2022) Shear strengthening of RC deep beams using glass chopped strand mat (GCSM) composite. *Case Stud Constr Mat* 16: 1–16. https://doi.org/10.1016/j.cscm.2022.e01018
18. Teng JG, Smith ST, Yao J, et al. (2003) Intermediate crack-induced debonding in RC beams and slabs. *Constr Build Mater* 17: 6–7. https://doi.org/10.1016/S0950-0618(03)00043-6
19. Rosenboom O, Rizkalla SH (2008) Experimental study of intermediate crack debonding in fiber-reinforced polymer strengthened beams. *ACI Struct J* 105: 41–50. https://doi.org/10.14359/19067
20. White TW, Soudki KA, Erki MA, et al. (2001) Response of RC beams strengthened with CFRP laminates and subjected to a high rate of loading. *J Compos Constr* 5: 153–162. https://doi.org/10.1061/(ASCE)1090-0268(2001)5:3(153)
21. Aram MR, Czaderski C, Motavalli M, et al. (2008) Debonding failure modes of flexural FRP-strengthened RC beams. *Compos Part B Eng* 39: 826–841. https://doi.org/10.1016/J.COMPOSITESB.2007.10.006
22. Khalifa A, Nanni A (2002) Rehabilitation of rectangular simply supported RC beams with shear deficiencies using CFRP composites. *Constr Build Mater* 16: 135–146. https://doi.org/10.1016/S0950-0618(02)00002-8
23. Dirar S, Lees JM, Morley CT, et al. (2013) Precracked reinforced concrete T-beams repaired in shear with prestressed carbon fiber-reinforced polymer straps. *ACI Struct J* 110: 855–865. https://doi.org/10.14359/51685838

24. Liu Q, Liu X, Chen R, et al. (2023) Experimental study on anchoring performance of short-lapped-rebar splices with pre-set holes and spiral hoops. *Metals* 13: 530. https://doi.org/10.3390/met13030530
25. Yang R, Yang Y, Zhang X, et al. (2023). An experimental study on secondary transfer performances of prestress after anchoring failure of steel wire strands. *Metals* 13: 1489. https://doi.org/10.3390/met13081489
26. Lam L, Hussain Q, Pimanmas A, et al. (2014) Shear strengthening of RC deep beams using glass chopped strand mat (GCSM). *Res Dev J* 24: 25–33.
27. Lam S, Khan AQ, Pimanmas A, et al. (2022) Shear strengthening of RC deep beams using glass chopped strand mat (GCSM) composite. *Case Stud Constr Mat* 16: e01018. https://doi.org/10.1016/j.cscm.2022.e01018
28. Bank LC, Arora D (2007) Analysis of RC beams strengthened with mechanically fastened FRP (MF-FRP) strips. *Compos Struct* 79: 180–191. https://doi.org/10.1016/j.compstruct.2005.12.001
29. Saingam P, Hlaing HH, Suwannatrai R, et al. (2023) Enhancing the flexural behavior of brick masonry walls with ferrocement overlays and low-cost anchors. *Case Stud Constr Mat* 19: e02558. https://doi.org/10.1016/j.cscm.2023.e02558
30. Hussain Q, Pimanmas A (2015) Shear strengthening of RC deep beams with openings using Sprayed Glass Fiber Reinforced Polymer Composites (SGFRP): Part 1. Experimental study. *KSCE J Civ Eng* 19: 2121–2133. https://doi.org/10.1007/s12205-015-0243-1
31. Rodsin K, Hussain Q, Parichatprecha R, et al. (2023) Monotonic and cyclic axial compressive responses of concrete specimens externally confined with different types of FRP composites: Experimental and analytical investigations. *Physica Scripta* 98: 105932. https://doi.org/10.1088/1402-4896/acf1d6
32. Nemeth I (1995) Hotavvezetekek hoszigeteles alatti korrozioja elleni vedelem. *Korroz Figy* 35: 36–38.
33. Zhang Z, Hsu CTT, Moren J, et al. (2004) Shear strengthening of reinforced concrete beams using carbon-fiber-reinforced polymer laminates. *J Compos Constr* 9: 158–169. https://doi.org/10.1061/(asce)1090-0268(2005)9:2(158)
34. American Society for Testing and Materials (ASTM) 2008 Standard test method for tensile properties of polymer matrix composite materials, ASTM D3039/D3039M-14 (West Conshohocken: American Society for Testing and Materials).

AIMS Press